Available online at www.sciencedirect.com

ScienceDirect

Physics Procedia 67 (2015) 1056 – 1061

Physics Procedia

25th International Cryogenic Engineering Conference and the International Cryogenic Materials Conference in 2014, ICEC 25–ICMC 2014

The thermal expansion and tensile properties of nanofiber-ZrW_2O_8 reinforced epoxy resin nanocomposites

Xinran Shan[a,b], Chuanjun Huang[b,*], Huihui Yang[b], Zhixiong Wu[b], Jingwen Li[b], Rongjin Huang[b], and Laifeng Li[b]

[a] *School of Materials Science and Engineering, Tianjin University, Tianjin 300072, China*
[b] *Key Laboratory of Cryogenics, Technical Institute of Physics and Chemistry, Chinese Academy of Sciences, Beijing 100190, China*

Abstract

Zirconium tungstate/epoxy (ZrW2O8/EP) nanocomposites were prepared and their thermal expansion properties were investigated within the temperature range of 4–300 K. Compared to unmodified epoxy resin, zirconium tungstate/epoxy composites lowers the thermal expansion coefficient (CTEs). The tensile strength was investigated at room temperature (300 K) and liquid nitrogen temperature (77 K). The fracture surfaces were examined by scanning electron microscopy (SEM). Results showed that the tensile strength and elongation at break increases with the increasing ZrW2O8 content.

Peer-review under responsibility of the organizing committee of ICEC 25-ICMC 2014

Keywords: ZrW2O8; nanofiber; epoxy resin; nanocomposites, thermal expansion; tensile

1. Introduction

Thermosetting epoxy resins have been widely employed as adhesives, sealants, and matrices of insulation material of superconducting magnets, due to their good electrical insulation properties, advantageous heat and chemical resistance, high elastic modulus, low density, strong bond ability, and convenient manufacturing process

* *Corresponding author. Tel.: +86-10-82543701; fax: +86-10-82543700*
E-mail address: cjhuang@mail.ipc.ac.cn

Peer-review under responsibility of the organizing committee of ICEC 25-ICMC 2014
doi:10.1016/j.phpro.2015.06.200

(Ueki 2005 and Kang 2001). However, epoxy resin exhibits a large coefficient of thermal expansion (CTE) of 40-80×10^{-6}/K, which limits their applications. When temperature changes, the volumetric shrinkage leads to internal stress and microcracks arise. For example, the structural failure occurred in cryogenic liquid-storage systems when the materials were not correctly designed. Therefore, development of epoxy resins with controlled thermal expansion is desired especially for cryogenic applications.

To attain desired thermal and mechanical properties, one approach is the addition of rigid micro- or nanofillers to a polymer (Chen 2010 and Li 2014). It is demonstrated that employing rigid fillers with a negative thermal expansion behavior can effectively reduce the CTE of the polymer composite at lower loadings (Huang 2010). A number of materials with large negative thermal expansion (NTE) are known. Among them, zirconium tungstate (ZrW2O8) has attracted growing research interest for its relatively strong and isotropic NTE over a wide temperature range (from 0.3 to 1050 K) (Xing 2005 and Kozy 2009). Therefore, ZrW2O8 is an attractive filler to tune the CTE of epoxy resin.

In this work, single crystalline ZrW2O8 nanofibers were prepared via a hydrothermal treatment followed by a sintering treatment (Chu 2011). Then zirconium tungstate/epoxy (ZrW2O8/EP) nanocomposites were prepared with different mass fractions of ZrW2O8 nanofiber. Thermal expansion properties were investigated within the temperature range of 4–300 K. The tensile properties of the nanocomposites were investigated at room temperature (300 K) and liquid nitrogen temperature (77 K). The fracture surfaces were examined by scanning electron microscopy (SEM).

2. Experimental

2.1. Synthesis of ZrW_2O_8 nanofibers

The precursor, $ZrW_2O_7(OH)_2 \cdot 2H_2O$ was prepared in a hydrochloric acid solutions in the presence of 1-butanol. First, solutions of $ZrOCl_2 \bullet 8H_2O$ and $Na_2WO_4 \bullet 2H_2O$ were mixed, then HCl and 1-butanol were added, and a white gel-like precipitate formed immediately. The mixtures were poured into the Parr bomb and then it was heated to 130 °C for 24 h. After cooling, the white precipitates were washed several times. Finally, it was sintered at 500 °C for 2 h and the $ZrW_2O_7(OH)_2 \cdot 2H_2O$ pieces changed to the ZrW_2O_8.

2.2. Preparation of ZrW_2O_8 epoxy nanocomposites

Epoxy resin and curing agent were mixed in a 250 ml beaker by the mass ratio of 100: 24. Then the ZrW_2O_8 was dispersed into the blends and sonicated for 30 min. The mixture was degassed by a vacuum pump at 45 °C for 1 h and then poured into a preheated mould. The sample was gelled at 80 °C for 24 h and cured at 130 °C for 12 h and cooled naturally with the oven to room temperature (RT). In this way, nanocomposites with different ZrW_2O_8 weight contents were prepared. The double-bell samples were then removed from the mould and used for further characterization.

2.3. Characterization

SEM experiments were carried out on a HITACHIS-4800 SEM. X-ray diffraction (XRD) analysis of ZrW_2O_8 particles were characterized using a Bruker AXS D8 Focus Diffractometer with Cu K_α radiation. The fracture surfaces were gold functionalized prior to investigation to improve conductivity. Tensile test was carried out by using a MTS-SUNS CMT 5000 test machine at both RT and 77 K with a cross-head speed of 1 mm/min. The specimens were prepared according to the ASTM D638 standard.

3. Results and discussion

The XRD pattern of precipitates is shown in Fig. 1 (a), matching the peaks of $ZrW_2O_7(OH)_2 \cdot 2H_2O$. After heating at 500 °C for 2 h, the XRD pattern of precipitates changed to Fig. 1. (b), which match peaks of the single phase of ZrW_2O_8 crystals. It is observed that all peaks of $ZrW_2O_7(OH)_2 \cdot 2H_2O$ disappeared after sintering treatment.

Fig. 2 (a) and Fig. 2 (b) show the SEM images of the ZrW_2O_8 nanofibers. As can be seen in Fig. 2 (a), the samples had average fiber widths of 20 to 40 nm. The fiber lengths were 600-800 nm. From Fig. 2 (b) we can see that the samples were agglomerated into bundles. The agglomerates were fairly mono-disperse (50-100 nm wide, 600-1000 nm long) and small enough to make them good candidates for incorporation into polymer composites.

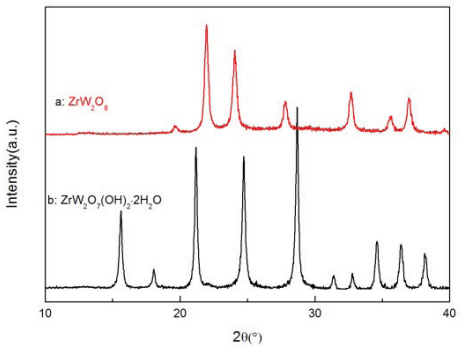

Fig. 1. XRD patterns of the $ZrW_2O_7(OH)_2 \cdot 2H_2O$ and the ZrW_2O_8.

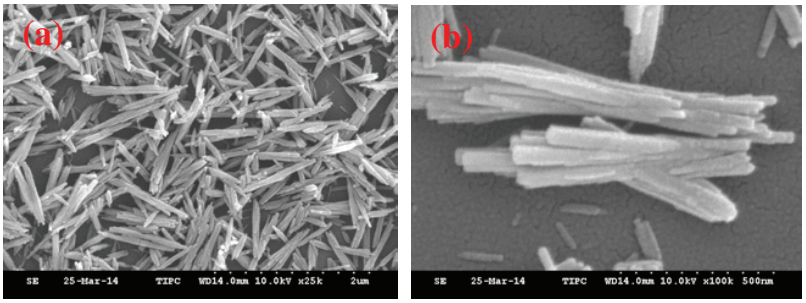

Fig. 2. SEM images of the ZrW_2O_8: (a) ZrW_2O_8 nanofibers and (b) ZrW_2O_8 nanofibers with high magnification.

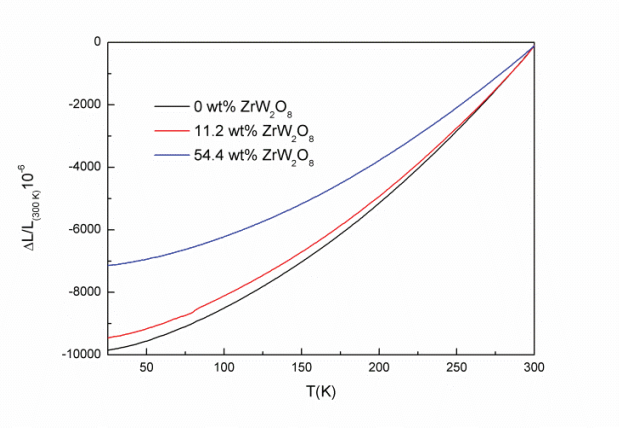

Fig. 3. Linear thermal expansion as a function of temperature of the nanocomposites.

Fig. 3 shows the linear thermal expansions ΔL/L (300K) of the ZrW_2O_8/EP nanocomposites. For comparison, the linear thermal expansion of unmodified epoxy resin is also shown. One can notice that the nanocomposites with ZrW_2O_8 material show lower thermal expansion than that the modified epoxy resin. In addition, it is noted that the linear thermal expansion ΔL/L (300 K) of nanocomposites decreases with the increase weight content of ZrW_2O_8 nanofiber. When considering the thermal expansion from room temperature to 77 K, it is observed that the average CTE of nanocomposites with 54.4 wt% NTE material is 25.9×10^{-6} K^{-1}, which is 27.5% lower than that of unmodified epoxy resin (35.787×10^{-6} K^{-1}). From the above data, it is evident that the NTE material filler plays a significant role in reducing the CTE of the epoxy resin.

Tensile properties of ZrW_2O_8/EP nanocomposites were measured at both RT and 77 K. The stress–strain curves of ZrW_2O_8/EP nanocomposites are shown in Fig. 4 at RT, the stress–strain curves show large plastic deformation prior to failure of the specimen, and the nanocomposites show a ductile behavior. When the temperature decreases to 77 K, the nanocomposites show a brittle behavior and increased strength. The tensile strength and Young's modulus of ZrW_2O_8/EP nanocomposites are shown in Fig. 5. Results show an increase trend in tensile strength at RT compared with unmodified epoxy resin. At 3.2 wt%, 4.4 wt%, 9.1 wt% and 11.2 wt% loadings of ZrW_2O_8, the tensile strength of the nanocomposites increase by 12.8%, 16.3%, 27.7% and 34.0%, respectively, in comparison to the unmodified epoxy resin.

The reinforcing effect of ZrW_2O_8 can be attributed to good dispersion and strong interfacial bonding between the ZrW2O8 and the epoxy resin. The tensile strength of the system at 77 K is much higher than that at RT. On the one hand, when the temperature decreased to 77 K, because of flexible chain structure and high thermal contraction of epoxy material, the networks of molecular chains shrink and the intermolecular forces become stronger (Chu 2011), thus a larger load will be needed to break the matrix. On the other hand, owing to different CTE between the ZrW_2O_8 and the polymer matrix, the interfacial bonding between the ZrW_2O_8 and the EP becomes stronger at cryogenic temperature, causing tight clamping of the ZrW_2O_8 by the matrix at low temperature. As a result, the strength of nanocomposites is significantly improved when the temperature is decreased to 77 K.

When the temperature decreases to 77 K, the tensile strength of the nanocomposites shows an increasing trend with increasing weight content of ZrW_2O_8 nanofibers. It is observed that the tensile strength of the nanocomposites increases by 2.2%, 9.3%, 12.2% and 32.1% compared to the unmodified matrix with the addition of 3.2 wt%, 4.4 wt%, 9.1 wt% and 11.2 wt%, respectively.

Fig. 6 shows fracture morphologies of the tensile fracture surface of nanocomposites. Certain increase of the matrix attached to the surface of the pulled out ZrW_2O_8 (Fig. 6 c and f) is observed, illustrating the strong interfacial bonding between ZrW_2O_8 and the matrix. The interfacial bonding is an important factor improving the mechanical properties of nanocomposites. Compared with the pure matrix, the fracture surface of nanocomposites shows significant increase in roughness, demonstrating the toughening effect of ZrW_2O_8 in matrix. And the fracture surface at 77 K is rougher than that at RT.

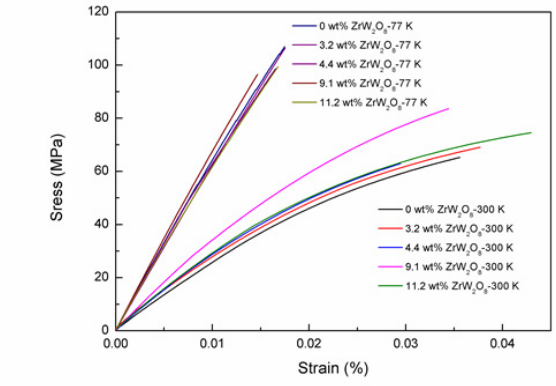

Fig. 4. Stress-strain curves of ZrW_2O_8/EP nanocomposites.

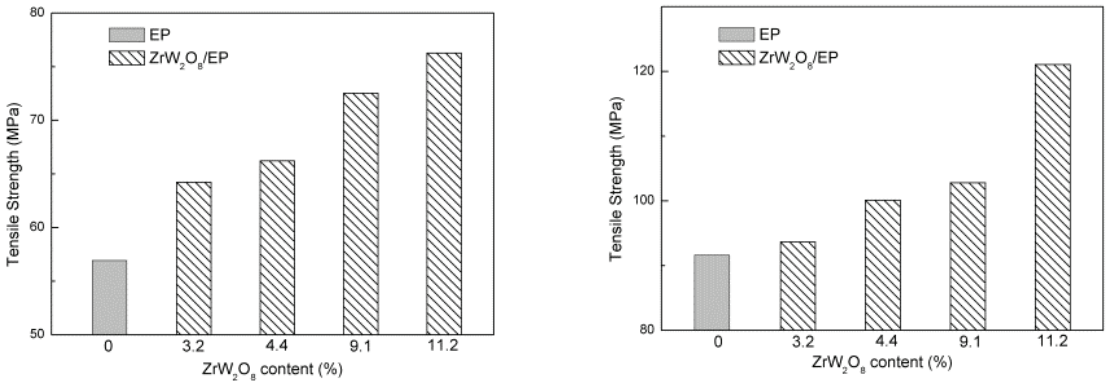

Fig. 5. Tensile strength of ZrW_2O_8/EP nanocomposites: (a) at RT and (b) at 77 K .

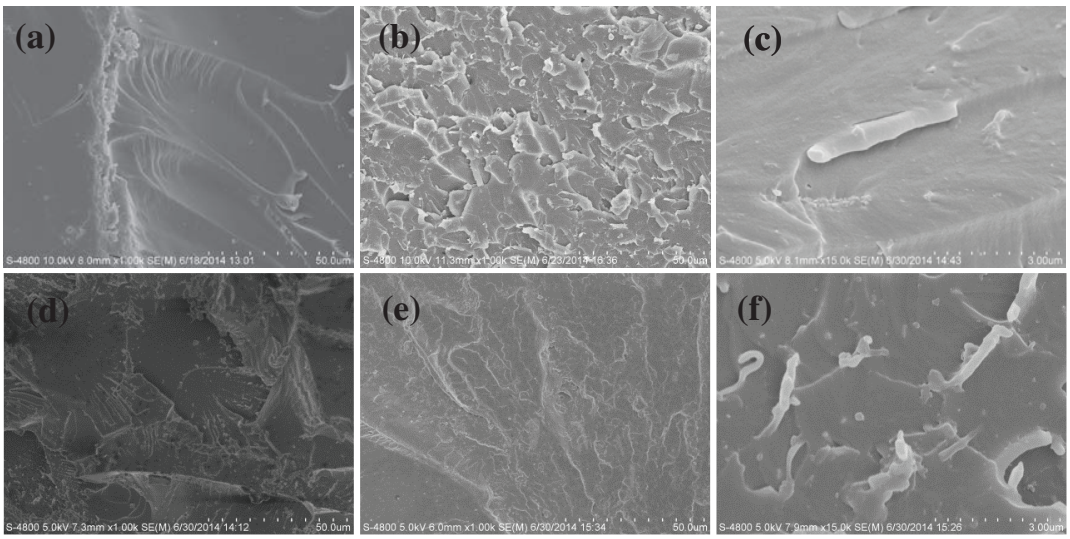

Fig. 6. SEM images of the fracture surface of ZrW_2O_8/EP with different content at different temperature:
(a) 0 wt% ZrW_2O_8-RT; (b) 11.2 wt% ZrW_2O_8-RT; (c) ZrW_2O_8-RT with high magnification;
(d) 0 wt% ZrW_2O_8-77 K; (e) 11.2 wt% ZrW_2O_8-77 K; (f) ZrW_2O_8-77 K with high magnification.

4. Conclusion

In this study, nanofiber-ZrW_2O_8/EP nanocomposites with different weight contents were prepared and it is observed that the CTEs of the nanocomposites decrease significantly with increase of nanofiber ZrW_2O_8. The nanocomposites containing ZrW_2O_8 nanofiber exhibit improved tensile strength compared to the unmodified epoxy resin and the CTEs of the nanocomposites can be tailored significantly. The nanocomposites containing ZrW_2O_8 exhibit improved tensile strength compared to the unmodified epoxy resin at both RT and 77 K.

Acknowledgment

This work was supported by the National Magnetic Confinement Fusion Science Program (grant No. 2011GB112003) and the National Natural Sciences Foundation of China (grant Nos. 51232004 and 51377156).

Reference

[1] Ueki T, Nishijima S and Izumi Y. Designing of epoxy resin systems for cryogenic use. Cryogenics 2005; 45(2):141-148.
[2] Kang S, Hong SI, Choe CR, Park M, Rim S, Kim J. Preparation and characterization of epoxy composites filled with functionalized nanosilica particles obtained via sol-gel process. Polym. 2001; 42:879-887.
[3] Chen IH, Wang CC, Chen CY. Preparation of carbon nanotube (CNT) composites by polymer functionalized CNT under plasma treatment. Plas. Process. Polym. 2010; 7:59-63.
[4] Li JW, Wu ZX, Huang CJ, Liu HM, Huang RJ, Li LF. Mechanical properties of cyanate ester/epoxy nanocomposites modified with plasma functionalized MWCNTs. Compos. Sci. Tech. 2014; 90:166-173.
[5] Huang RJ, Chen Z, Chu XX, Wu ZX, Li LF. Preparation and thermal properties of epoxy composites filled with negative thermal expansion nanoparticles modified by a plasma treatment. J. Compos. Mater. 2010; 45(16):1675-1682.
[6] Xing QF, Xing XR, Yu RB, Du L, Meng J, Luo J, Wang D, Liu G. Single crystal growth of ZrW2O8 by hydrothermal route. J. Cryst. Growth. 2005; 283:208-214.
[7] Kozy LC, Tahir MN, Cora LC, Tremel W. Particle size and morphology control of the negative thermal expansion material cubic zirconium tungstate. J. Mater. Chem. 2009; 19:2760-2765.
[8] Wu HC, Rogalski M, Kessler MR. Zirconium tungstate/epoxy nanocomposites: effect of nanoparticle morphology and negative thermal expansivity. Appl. Mater. Inter. 2013; 5: 9478-9487.
[9] Chu XX, Huang RJ, Yang HH, Wu ZX, Lu JF, Zhou Y, Li LF. The cryogenic thermal expansion and mechanical properties of plasma modified ZrW2O8 reinforced epoxy. Mater. Sci. Eng. A 2011; 528:3367-3374.